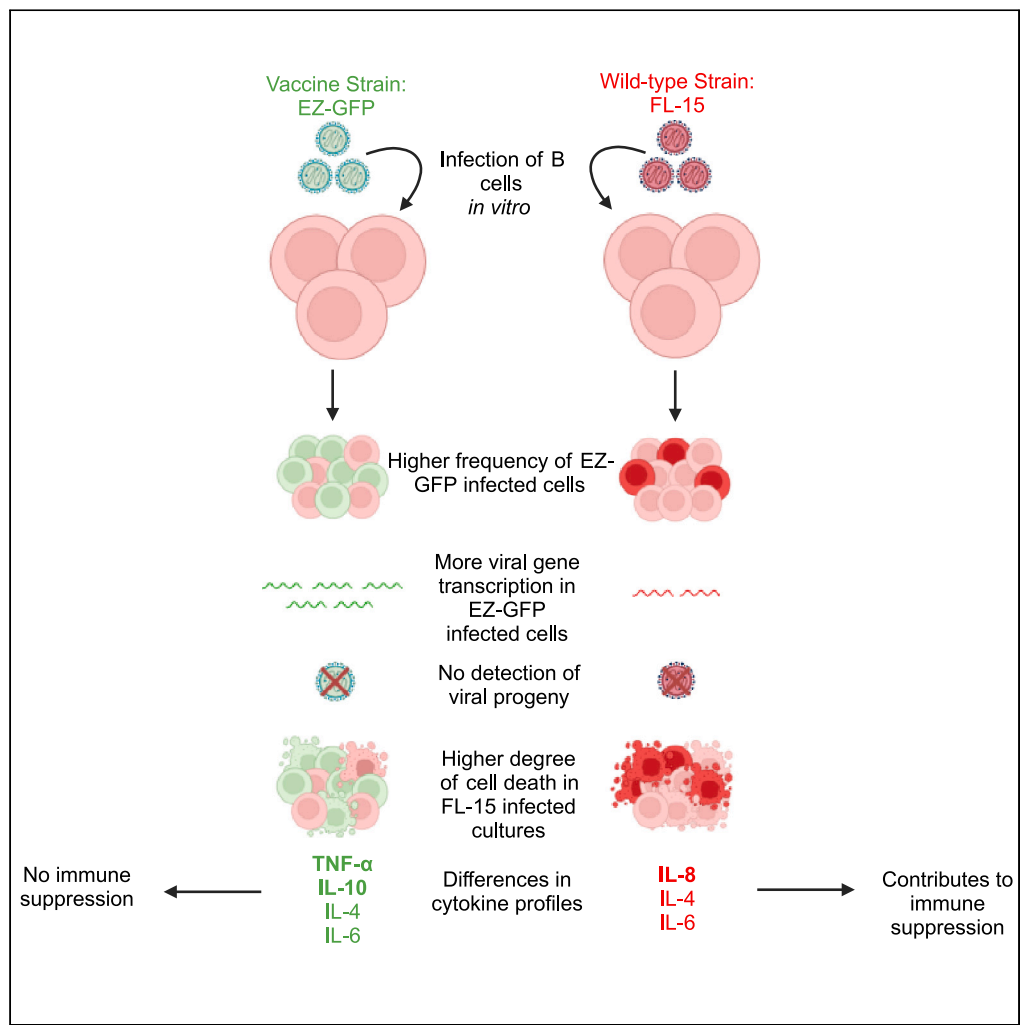


Article

# Characterizing infection of B cells with wild-type and vaccine strains of measles virus



Logan Melot,  
Bettina Bankamp,  
Paul A. Rota,  
Melissa M.  
Coughlin

lmelot@emory.edu

**Highlights**

Infection frequency differs in EZ-GFP and FL-15 infected B cell cultures

Progeny virus not produced following MeV infection of B cell cultures *in vitro*

Increased cell death in FL-15 compared to EZ-GFP infected B cell cultures

Cytokine profile differs between FL-15 and EZ-GFP infected B cell cultures

Melot et al., iScience 26, 107721  
October 20, 2023  
<https://doi.org/10.1016/j.isci.2023.107721>



## Article

## Characterizing infection of B cells with wild-type and vaccine strains of measles virus

Logan Melot,<sup>1,2,3,\*</sup> Bettina Bankamp,<sup>1</sup> Paul A. Rota,<sup>1,2</sup> and Melissa M. Coughlin<sup>1</sup>

## SUMMARY

**Acute infection with measles virus (MeV) causes transient immunosuppression often leading to secondary infections. MeV infection of B lymphocytes results in changes in the antibody repertoire and memory B cell populations for which the mechanism is unknown. In this study, we characterize the infection of primary B cells with wild-type and vaccine strains of MeV. Vaccine-infected B cells were characterized by a higher percentage of cells positive for viral protein, a higher level of viral transcription and reduced cell death compared to wild-type infected cells, regardless of B cell subtype. Vaccine-infected cells showed more production of TNF- $\alpha$  and IL-10 but less production of IL-8 compared to wild-type infected cells. IL-4 and IL-6 levels detected were increased during both vaccine and wild-type infection. Despite evidence of replication, measles-infected B cells did not produce detectable viral progeny. This study furthers our understanding of the outcomes of MeV infection of human B cells.**

## INTRODUCTION

Measles virus (MeV) is an enveloped negative sense RNA virus in the *morbillivirus* genus of the family *Paramyxoviridae*. Measles presents with a maculopapular skin rash, a fever above 38.3°C, cough, coryza, and conjunctivitis.<sup>1</sup> The case fatality rate for measles can range from 0.2 to 29.1% depending on the epidemiologic setting.<sup>2</sup> A highly effective vaccine for the virus was developed in 1963, and despite the estimated 31.7 million lives saved worldwide through measles vaccination,<sup>3</sup> there were still 149,796 cases and an estimated 60,700 deaths in 2020.<sup>4</sup> The COVID-19 pandemic has further exacerbated the threat of MeV globally as surveillance and vaccination coverage have declined, with a 2% decrease in first dose measles vaccination, and a 1% decrease in second dose vaccination globally. This coincided with a 23% decrease in countries with >90% first dose measles vaccine coverage.<sup>4</sup>

Individuals are infected via the respiratory route through the inhalation of respiratory droplets. MeV is lymphotropic, initially targeting signaling lymphocytic activation molecule F1 (SLAMF1, CD150)-expressing alveolar macrophages and dendritic cells in the respiratory tract followed by transmission to SLAM-expressing B and T cells in the surrounding bronchus-associated lymphoid tissue.<sup>5</sup> Infected cells migrate to draining lymph nodes, further replicating in B and T cells leading to lymphopenia and a generalized prolonged immune suppression.<sup>6,7</sup> Following replication in the lymph nodes, MeV disseminates to the periphery, infecting nectin-4+ epithelial cells, leading to the characteristic maculopapular rash and allowing for spread through infectious respiratory droplets.<sup>8,9</sup> Measles-associated immune suppression is observed only following infection and is not observed after vaccination with the measles, mumps, and rubella (MMR) vaccine.<sup>10</sup> MeV-induced immune suppression is characterized by increased secondary infections which are a major cause of morbidity and mortality in children.<sup>7</sup> Children with measles are more likely to require prescription antivirals and antibiotics in the months and years following MeV infection.<sup>11</sup> The mechanism by which MeV causes immune suppression is not fully understood. Studies performed *in vitro* have demonstrated immune cell dysfunction in dendritic cells and CD8<sup>+</sup> T cells.<sup>6,12</sup> B cells are highly targeted in non-human primate models of measles infection, accounting for approximately 20–30% of infected PBMCs.<sup>13,14</sup> Importantly, infected individuals have changes in the frequency of T cell subtypes and a decrease in class-switched memory B cells, resulting in a decline in circulating non-MeV specific antibodies and an altered antibody repertoire accompanied by a decrease in B cell clonal diversity.<sup>15,16</sup> The targeting of and changes in B cell-associated immune profiles suggests that B cells could play a significant role in measles induced immune dysregulation. This study aims to better understand the characteristics of B cell infection with vaccine (Edmonston-Zagreb strain, EZ) and wild-type (MVs/Florida.USA/12.15 [D8], FL-15) strains of MeV. EZ expressing GFP (EZ-GFP) was used as a representative for vaccine viruses because the Edmonston-Zagreb vaccine strain has been the most widely used measles vaccine strain globally since its licensure in 1967.<sup>17</sup> A MeV isolate of genotype D8, FL-15, was used as a representative wild-type virus because >50% of sequences reported to the Measles Nucleotide Surveillance (MeaNS) sequence database were genotype D8

<sup>1</sup>Viral Vaccine Preventable Diseases Branch, Division of Viral Diseases, National Center for Immunization and Respiratory Diseases, Centers for Disease Control and Prevention, Atlanta, GA 30333, USA

<sup>2</sup>Emory University, Atlanta, GA 30333, USA

<sup>3</sup>Lead contact

\*Correspondence: [lmelot@emory.edu](mailto:lmelot@emory.edu)

<https://doi.org/10.1016/j.isci.2023.107721>



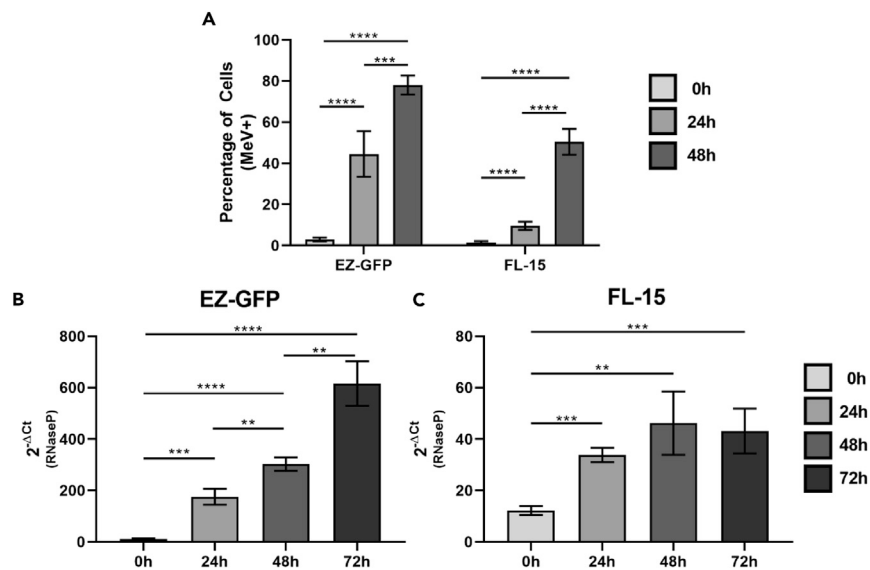


**Figure 1. MeV protein expression and transcription in infected BJAB cells**

(A–C) Measles hemagglutinin (H) expression in FL-15 and GFP expression in EZ-GFP infected BJAB cells were analyzed by flow cytometry (A) ( $n = 5$ ). Transcription of MeV N gene normalized to RNaseP was measured by rRT-PCR in cells infected with EZ-GFP (B) and FL-15 (C) ( $n = 3$ ). Statistics were determined using multiple t-tests. Error bars represent standard deviation (\*\* =  $p < 0.01$ , \*\*\* =  $p < 0.005$ , \*\*\*\* =  $p < 0.001$ ).

in 2018 and this percentage has continued to increase in recent years.<sup>18–20</sup> We assessed viral transcription and protein production in B cell subtypes and the outcome of infection of B cells including cell survival, production of viral progeny, and cytokines to further our understanding of the characteristics of B cell infection with MeV.

## RESULTS

### MeV protein production and gene transcription in BJAB cells

BJAB cells, an Epstein-Barr virus-negative human B cell lymphoma cell line, were used to as a model for MeV infection of B cells *in vitro*. Viral N gene transcription and protein production were measured in BJAB cells following infection at an MOI of 1 with the EZ-GFP or FL-15 strains of MeV. GFP was used to measure infection with the vaccine strain and H protein expression was used to measure infection with FL-15. The levels of viral protein production following detection of GFP, or cell surface H expression were equivalent in EZ-GFP-infected BJAB cells, demonstrating that detection of GFP or H could be used to measure viral protein expression for EZ-GFP (Figure S2). GFP was expressed in 44.6% of EZ-GFP-infected BJAB cells at 24 h and 78% at 48 h, while H protein was expressed in 9.6% of FL-15-infected cells at 24 h and 50.4% at 48 h (Figure 1A).

Real-time RT-PCR indicated that viral lysates had low levels N gene mRNA (data not shown) which accounts for detection of N gene RNA at the 0-h timepoint. EZ-GFP infection resulted in a 15.2-fold increase in N gene mRNA transcription from 0 to 24 h. N gene transcription in EZ-GFP infected cells continued to increase between 24 and 72 h post-infection with a 1.73-fold change from 24 to 48 h, and a 2.03-fold change from 48 to 72 h (Figure 1B). Compared to EZ-infected cells, FL-15-infected BJAB cells had significantly lower levels of N gene transcription. Additionally, unlike transcription in EZ-GFP-infected BJAB cells which continued to increase over the time-course, transcription in FL-15-infected cells increased significantly only in the first 24 h, (2.78-fold change from 0 to 24 h), followed by a modest but not significant increase at 48 h (1.36-fold change from 24 to 48 h), and no detectable increase from 48 to 72 h (Figure 1C). Increased mRNA transcription and protein production demonstrated that BJAB cells allow for viral transcription and protein production following infection with EZ-GFP or FL-15 strains of MeV. However, infection with FL-15 resulted in a lower proportion of infected cells and less transcription and protein production.

### Analysis of viral protein expression in infected primary B lymphocytes *in vitro*

MeV infection characteristics in primary cells were assessed in B cells isolated from healthy human donors. A representative gating strategy to measure viral protein production in negatively selected CD19<sup>+</sup> live B cells by flow cytometry is shown (Figure 2A). Cells stained immediately after infection (0 h) were used to determine the lower boundary of gating for infected cells as measured by viral GFP or H expression for vaccine and wild-type virus, respectively (Figure 2B). Two separate experiments were performed to measure viral protein expression at 0 and 24 h (Figure 2C) and 0 and 48 h post-infection (Figure 2D) due to the limited B cell recovery from whole blood. At 24 h post-infection, 14.4% of EZ-GFP-infected B cells expressed GFP (Figure 2C). At 48 h post-infection, the percentage of GFP-expressing B cells increased to 26.1% (Figure 2D). FL-15 infected B cells demonstrated a lower percentage of infected cells at 24 h (7.7% of B cells expressing MeV-H), and no significant increase in the proportion of infected cells at 48 h post-infection (8.23% of B cells expressing MeV-H) (Figure 2D). Both EZ-GFP- and

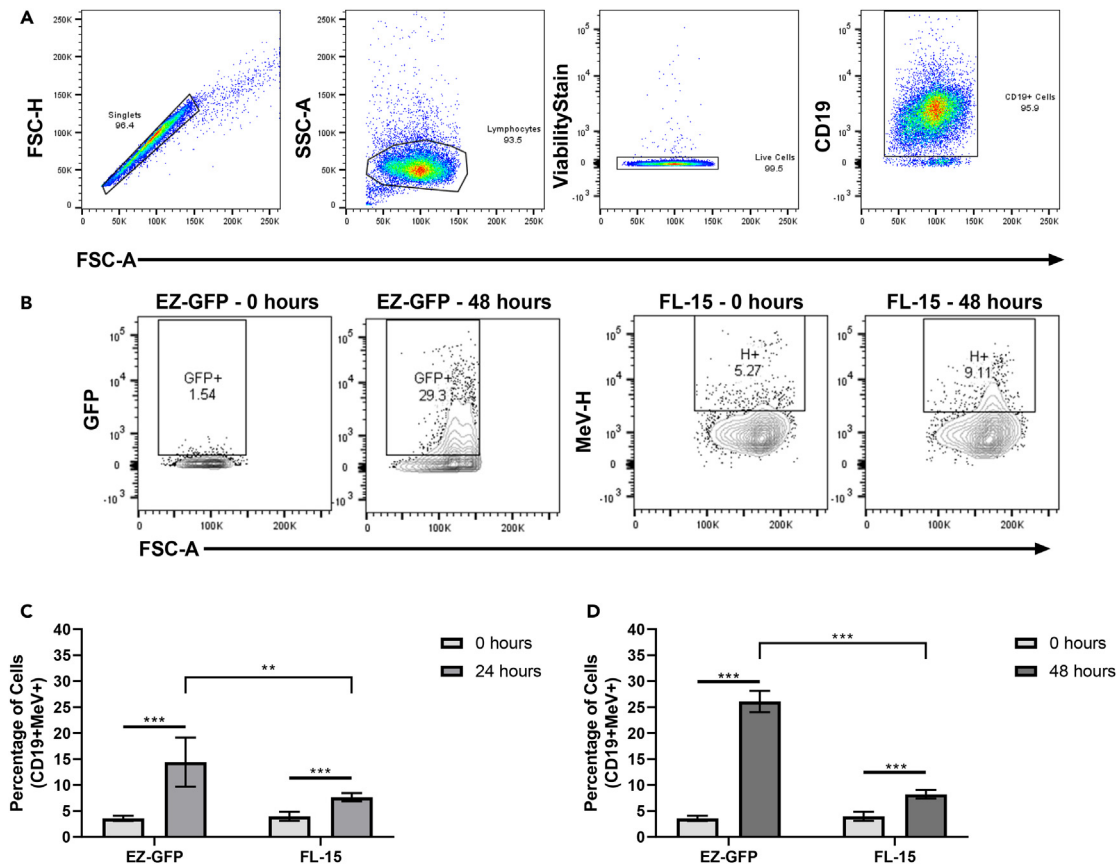


**Figure 2. MeV protein expression in infected B lymphocytes**

(A–D) B cells isolated from whole blood of two healthy human donors were infected with EZ-GFP or FL-15. Example gating strategy used for analysis, cells were gated on singlets, lymphocytes, viability, and CD19 (A). The number of infected cells was determined relative to cells stained at 0 h-post infection (B). For MeV vaccine infected B cells, GFP expression was measured at 0 h and 24 h (C) and 0 h and 48 h (D) in two separate infections, each performed in triplicate. Surface expression of MeV H protein in wild-type MeV infected cells was measured with a mixture of CV1/CV4 antibodies directed against the H protein. Expression was measured at 0 h and 24 h (C) and 0 h and 48 h (D) in two separate infections, each performed in triplicate. Results from both donors are combined in each figure C and D. Statistical analyses were also performed to assess differences between EZ-GFP and FL-15 at 24 (C) and 48 h (D). Statistics were determined using multiple t-tests. Error bar represents standard deviation ( $n = 4$ , \*\*\* =  $p < 0.005$ , \*\* =  $p < 0.01$ ).

FL-15-infected B cells showed increased viral protein expression; however, this increase appears limited to the first 24 h in FL-15 infected cells with minimal differences in the mean percentage of infected cells after 24 h.

### Transcription of MeV N gene in infected primary B cells

Differences in viral gene transcription in B cells infected with EZ or FL-15 at an MOI of 1 were assessed by rRT-PCR targeting N gene mRNA in B cells from two healthy human donors. At 24 h post-infection, there was a comparable increase in MeV N gene transcription in B cells from both donors infected with EZ-GFP, with a 1.48-fold increase in N gene transcript normalized to RNaseP in B cells from Donor 1 (Figure 3A) and a 1.45-fold increase in cells from Donor 2 (Figure 3B). However, FL-15-infected B cells showed no significant increase in N gene transcription from 0 to 24 h in B cells from either donor (Figures 3A and 3B). While detectable transcription increased in B cells from both donors 48 h after infection with vaccine virus, cells from Donor 1 demonstrated greater increase in transcription (4.37-fold) compared to B cells from Donor 2 (2.5-fold) (Figures 3C and 3D). This difference between donors was not detected in FL-15-infected B cells and both donors demonstrated a similar 2.4-fold increase in N gene transcription at 48 h post-infection (Figures 3C and 3D). These data show that B cells infected with FL-15 and EZ-GFP strains of MeV showed an increase in viral transcripts; however, FL-15 transcription occurred later post-infection and to lower abundance compared with EZ-GFP.

### Infection of naive and memory B cell subtypes

Preferential infection of B cell subtypes by MeV was evaluated by infecting freshly thawed B cells from STEMCell from two donors with EZ-GFP and FL-15. Results were analyzed according to the gating strategy shown in Figures 4A and 4B. MeV infection of freshly isolated and frozen

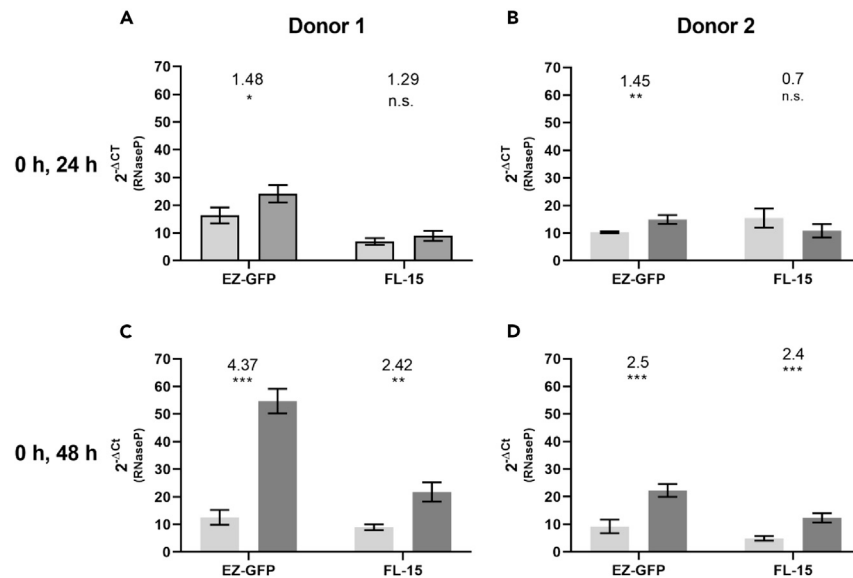


**Figure 3. MeV N gene transcription following *in vitro* infection of human B lymphocytes**

(A–D) B cells isolated from fresh blood were infected and assessed for N gene expression. N gene expression was measured via rRT-PCR using RNA from B cells infected with EZ-GFP or FL-15. N gene transcription at 0 h and 24 h (A, B) and at 0 h and 48 h (C, D) was normalized to RNaseP in two separate experiments. Fold change in N gene transcription is shown above columns. Infections were performed in triplicate in cells isolated from two healthy donors in two separate infections. Error bars represent standard deviation (n = 4, significance was determined by Student's t test \* = p < 0.05, \*\* = p < 0.01, \*\*\* = p < 0.005).

B cells from donors was found to be equivalent (Figure S3). Memory cell subtypes were determined based on IgD and CD27 expression. CD27<sup>+</sup> single positive cells were identified as switched memory cells, CD27+IgD + double-positive cells were identified as non-switched memory cells, IgD+ single positive cells were identified as naive cells, and cells that expressed neither marker were identified as double-negative.<sup>21</sup> GFP or H expression was evaluated in the B cell subtypes as a marker of MeV infection, with the lower boundary of the gate determined based on cells stained at 0 h post-infection (Figure 4B). Cells of all B cell subtypes infected with EZ-GFP showed a significant increase in the percentage of GFP-expressing cells from 0 to 24 (Figure 4C). Between 24 and 48 h post-infection naive, switched memory and double-negative B cell subtypes showed a significant increase in the percentage of GFP positive cells following EZ-GFP infection (Figure 4C). There was no significant increase in the frequency of infected cells from 0 to 24 h in cells infected with FL-15; however, a significant increase was detected from 24 to 48 h in all four subtypes (Figure 4D). Preferences for specific subtypes was determined by comparing frequency of infected cells between each subtype using multiple t-tests. At 24 h, there was no detectable difference between subtypes in EZ-GFP infected cells (Figure 4E). Non-switched memory cells had a significantly lower percentage of infected cells at 48 h when compared to naive, switched memory, and double-negative cells (Figure 4E). In FL-15 infected B cells, the only significant difference in the frequency of infected cells was observed between switched memory and double-negative subtypes, with double-negative cells showing a slightly lower frequency of infection (Figure 4F). At 48 h post-infection there were no detectable differences in the frequency of infected subtypes following infection with FL-15 (Figure 4F). These data show that all subtypes are infected at similar frequencies but there is slightly reduced infection in non-switched memory cells at 48 h with EZ-GFP and for double-negative cells at 24 h post-infection with FL-15.

### Production of MeV from infected B cells

Viral transcription and protein expression were detected in B cells over 48 h post-infection; therefore, the production of infectious viral particles from B cells was evaluated. Supernatants and lysates were collected at 0, 24 and 48 h post-infection from B cells infected with either EZ-GFP or FL-15 and titrated on Vero/hSLAM cells. Viral titers did not increase over input (0 h post-infection) in either EZ-GFP (Figure 5A) or FL-15 (Figure 5B) infected cells. Residual inoculum from an infection done at an MOI of 1 may mask small increases in viral titer. Potential small increases in viral titer were assessed by the removal of viral inoculum after 2 h of infection from BJAB cells infected at an MOI of 1, followed by incubation for an additional 48 h. Like the results in B lymphocytes, no detectable increase in viral titer over input was observed in EZ-GFP (Figure 5C) or FL-15 (Figure 5D) infected BJAB cells following inoculum removal. MeV infection of BJAB cells at a low MOI of 0.001 was evaluated to detect increases in viral titer over an extended time-course; however, similar results in viral transcription, protein expression, and the lack of detection of viral progeny above input were observed (Figure S4). Despite MeV protein expression and N gene transcription in MeV-infected B cells, there was no detectable increase in infectious virus in the supernatant nor in the cell lysate following 48 h of infection with EZ or FL-15.

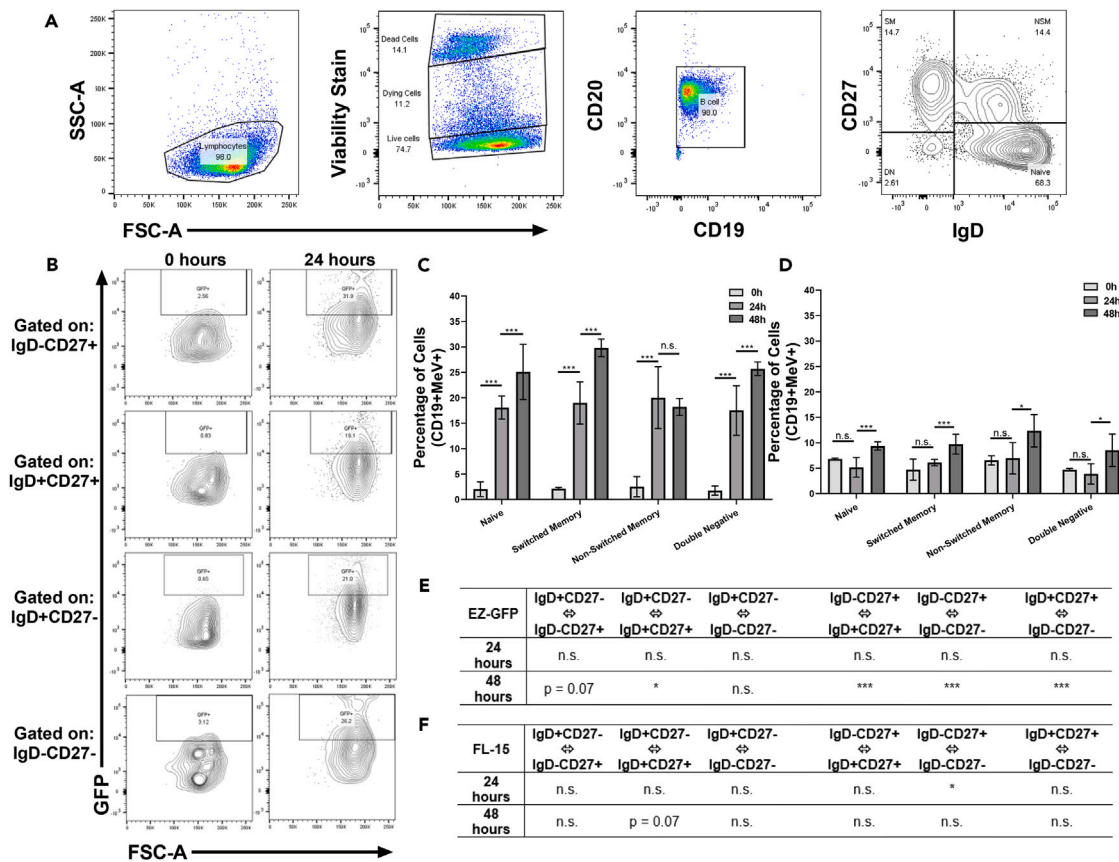


**Figure 4. MeV protein expression in B cell subtypes following infection**

(A–F) Freshly thawed B cells from human donors, provided by STEMCell, were infected *in vitro*. Cells were gated on live CD19<sup>+</sup>CD20<sup>+</sup> B cells and subdivided into memory and naive subtypes by CD27 and IgD expression (A) IgD-CD27<sup>+</sup> (Switched Memory), IgD+CD27<sup>+</sup> (Non-switched Memory), IgD+CD27<sup>-</sup> (Naive), IgD-CD27<sup>-</sup> (Double-Negative). MeV H protein or recombinant GFP expression corresponding to infected cells was evaluated in each B cell subtype with the gate set based infected cells stained at 0 h. Expression of GFP in EZ-GFP infected B cell subtypes (C) and hemagglutinin (H) in FL-15 infected B cell subtypes (D) was evaluated by the example gating strategy of B cells 0 and 48 h post-infection (B). Statistical analyses were performed to assess differences in infections between subtypes during infection with EZ-GFP (E) or FL-15 (F). Infections were performed in two separate donors in triplicate. Error bars represent standard deviation and significance was determined by multiple t-tests (n = 4. n.s. = non-significant, \*\*\*\* = p < 0.0001, \*\*\* = p < 0.005, \*\* = p < 0.01, \* = p < 0.05, ↔ = conditions compared in the statistical analysis).

### Assessment of cellular viability in B cells during infection with MeV

Cellular viability was evaluated in infected B cells (MOI of 1) at 0, 24, and 48 h (Figure 6) to assess cell death in EZ-GFP and FL-15-infected cells using the gating strategy shown (Figure 4A). Loss of viability was determined as dead or dying cells. An overall 10.7% loss of viability in B cells from being in culture was detected at 24 h and 16.5% at 48 h. An increase in loss of viability was observed in EZ-GFP infected cells compared to uninfected cells with 29.3% dead or dying cells at 24 h post-infection; however, this did not continue to increase significantly at 48 h post-infection (27.9%). FL-15 infected cells had less cell death at 24 h (15.1%) when compared with vaccine infected cells. However, FL-15-infected cells had a significantly higher loss of viability (43.9%) than EZ-GFP-infected cells at 48 h, despite higher levels of viral gene transcription and protein expression in EZ-GFP infected cells. We further investigated viability loss in B cell subtypes and noted significant loss of viability in FL-15 infected naive B cells, accounting for the majority subtype within the B cell population of isolated peripheral blood cells, with elevated levels of cell death noted in other memory subtypes at 48 h (Figure S5).

### Cytokine production in B cells infected with MeV

Cytokine expression was evaluated in EZ-GFP or FL-15 infected B cells provided by STEMCell (MOI of 1) at 24- and 48-h post-infection (Figures 7A–7E). A significant increase in most cytokines was measured in EZ-GFP infected cells compared to mock infected cells stimulated with Vero/hSLAM lysate (Figure S6) at 24 and 48 h post-infection. However, fewer cytokines (IL-6, IL-8, and IL-10) were expressed at significantly higher levels (p < 0.05) compared to mock infected cells at these same timepoints in FL-15 infected cells. TNF- $\alpha$ , IL-4, IL-6, and IL-8 continued to increase in the supernatant of EZ-GFP infected cells between 24 and 48 h post-infection (p < 0.05) (Figures 7A–7D), but this was not observed for IL-10 expression (Figure 7E). A significant increase (p < 0.05) in IL-8 expression was detected from 24- to 48 h

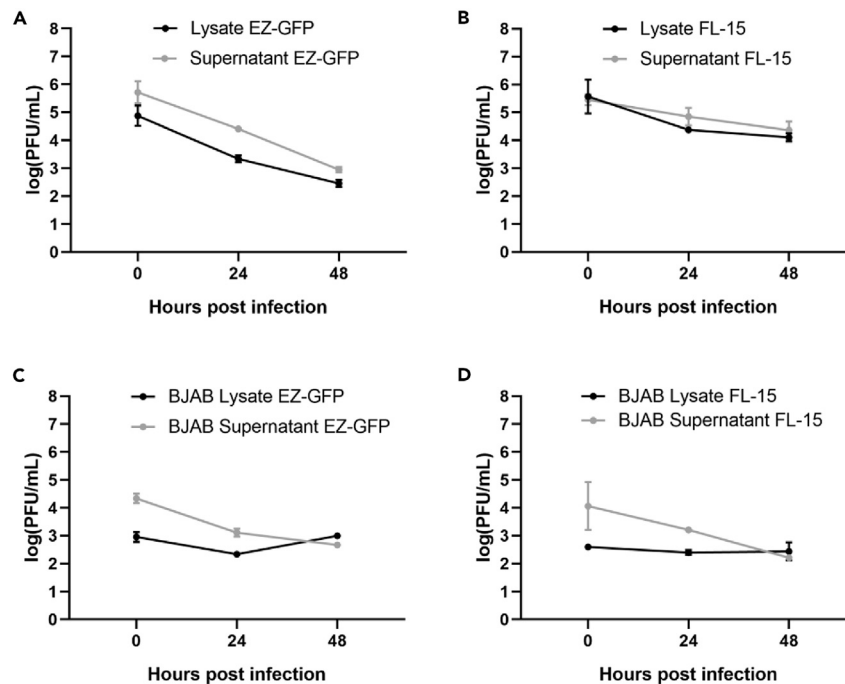


**Figure 5. Measurement of progeny MeV in B lymphocytes at 48 h infection**

(A–D) B cells were isolated from fresh blood and infected. Viral titers in supernatant or lysate from B cells (panels A and B) or BJAB cells (panels C and D) infected with EZ-GFP (panels A and C) or FL-15 (panels B and D) were measured by endpoint dilution in using Vero/hSLAM cells. Virus inoculum was not removed from B cells (A and B) but viral inoculum was removed after 2 h of incubation from BJAB cells (C and D). Viral titer was plotted as the log PFU/mL. Error bars represent standard deviation. Experiments were performed in two separate donors in duplicate (n = 4).

post-infection with FL-15 infected cells (Figure 7D), and a significant decrease ( $p < 0.05$ ) in production of IL-10 was detected (Figure 7E), concentrations of all other cytokines evaluated did not change in the supernatant of FL-15 infected cells between 24 and 48 h post-infection. The level of TNF- $\alpha$  measured in EZ-GFP infected cells was significantly higher ( $p < 0.05$ ) than in FL-15 infected cells at both 24 and 48 h post-infection, with IL-10 also demonstrating significantly higher ( $p < 0.05$ ) levels in EZ-GFP infected cells at 48 h post-infection (Figures 7A and 7E). A single cytokine, IL-8, demonstrated significantly higher ( $p < 0.05$ ) expression in FL-15 infected cells compared to EZ-GFP infected cells at both 24 and 48 h post-infection (Figure 7D).

## DISCUSSION

MeV targets and induces changes in B cell repertoires *in vivo* [8] and B cells are susceptible to infection *in vitro*,<sup>22</sup> but infection of human B cells with MeV has not been fully characterized. Our study showed higher levels of viral transcription and protein expression in EZ-GFP infected BJAB and primary B cells at 24 and 48 hours-post-infection compared to FL-15 infected cells. Viral transcription and the percentage of infected cells continued to increase in EZ-GFP infected cells, but not FL-15 infected cells between 24 and 48 h. Increased EZ-GFP infection was observed in all B cell subtypes. Similar to previously published results,<sup>14</sup> MeV comparably targeted naive and memory cells. When the memory B cell population was further subtyped, EZ-GFP appeared to target non-switched memory cells at 48 h post-infection less than other B cell subtypes, whereas FL-15 appeared to target non-switched memory cells at a slightly higher, though not significant ( $p = 0.07$ ) frequency. Non-switched memory cells, defined as IgD+CD27<sup>+</sup> are circulating marginal zone (MZ) B cells<sup>23</sup> which are responsible for an initial burst of broadly reactive IgM antibodies after exposure to antigen.<sup>24</sup> Preferential targeting of non-switched memory cells *in vivo* may contribute to the increase in secondary infections that is observed following infection with wild-type MeV.<sup>7</sup> Understanding the impact of infection on MZ B cells during *in vivo* infection could help elucidate mechanisms that contribute to immune suppression.

While there is evidence of infection in target B cells, no detectable changes in viral titer above input were observed in the supernatant or infected cell lysate. There were no measles specific antibodies detected in the supernatant from infected cells, demonstrating that the lack of viral progeny was not due to the presence of neutralizing antibodies (data not shown). This observation suggests that measles viral components are spreading via non-canonical methods in B cells. The spread of MeV through non-canonical pathways has been documented in other immune and non-immune cells to occur through mechanisms such as the formation of a “virological synapse”, actin mediated polarization, and spread of viral nucleocapsid through pore formation, and are likely to play a role in B cell infections.<sup>8,25,26</sup>

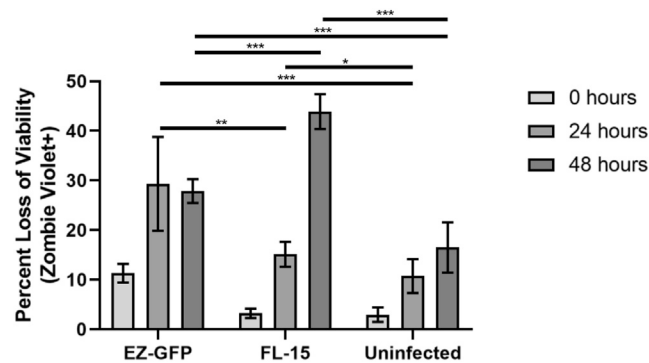


**Figure 6. Cell viability following MeV infection**

B cells isolated from whole blood of two healthy human donors were infected with EZ-GFP and FL-15 with infections performed in triplicate. Infected cells were assessed for viability using a fluorescent amine-reactant dye. The gating strategy from Figure 4A was used to determine boundaries for loss of viability. Loss of viability included dying and dead cells measured at 0, 24, and 48 h in infected and uninfected cells. Error bars represent standard deviation. Statistics were determined using multiple t-tests ( $n = 4$ ,  $*** = p < 0.001$ ,  $** = p < 0.01$ ,  $* = p < 0.05$ ).

Infected BJAB cells demonstrated similar levels and patterns of viral replication as primary cells. BJAB cells had higher frequencies of infected cells for both EZ-GFP and FL-15 when compared to primary cells. The difference in the time course of infection between EZ-GFP and FL-15 in primary B cells was also reflected in infected BJAB cells. Previous studies have used an infection enhancing molecule known as PHCSK4 when evaluating MeV infection of B cells<sup>27</sup>; however, little enhancement of infection was observed (data not shown). Similar to

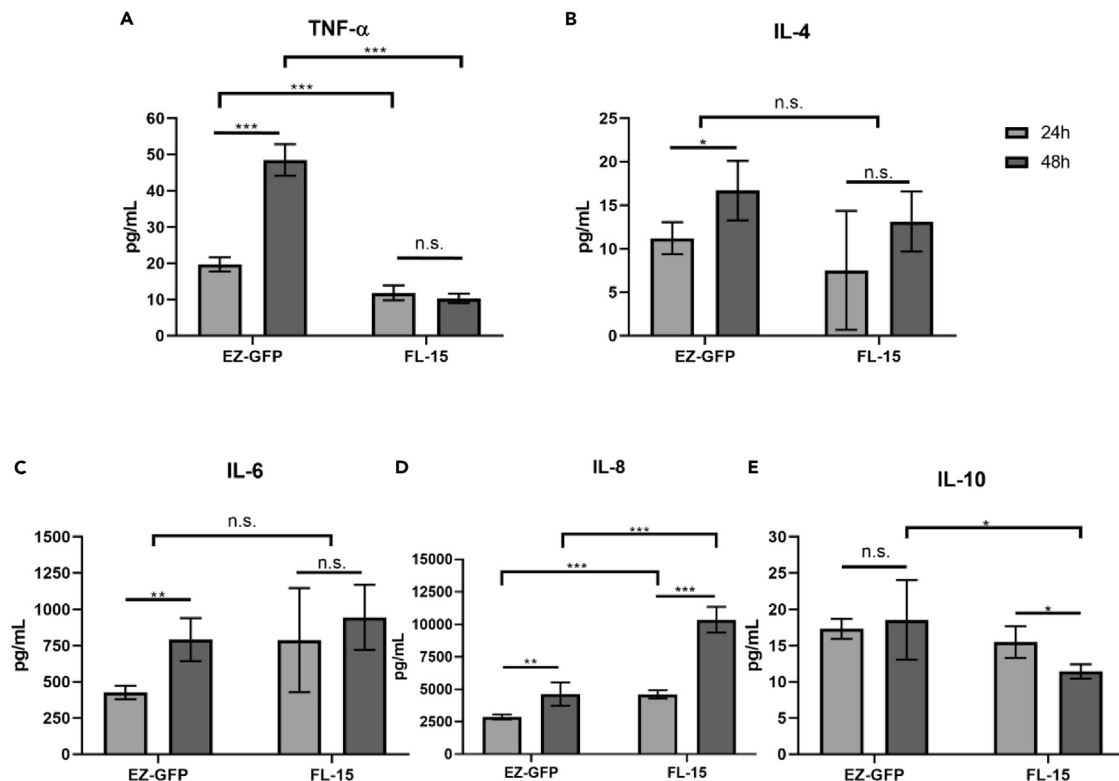


**Figure 7. Cytokine protein production in B cells following MeV infection**

(A–E) Previously frozen B cells (STEMCell) from two healthy donors were infected with EZ-GFP or FL-15 at an MOI of 1. Supernatants were collected and stored at  $-80^{\circ}\text{C}$ . Supernatants from 24 h post-infection and 48 h post-infection were assessed for TNF- $\alpha$  (A), IL-4 (B), IL-6 (C), IL-8 (D), and IL-10 (E) using a multiplex bead based Luminex assay. Statistical differences between each condition were assessed at individual timepoints using multiple t-tests between each condition and from 24 to 48 h post-infection. Stimulation and infection were performed in two separate donors in duplicate ( $n = 4$ ,  $*** = p < 0.001$ ,  $** = p < 0.01$ ,  $* = p < 0.05$ ).

primary cells, infected BJAB cells did not generate an increase in infectious particles above input. The results from these studies suggest that infection of BJAB cells can potentially be used to inform future experiments for infection of primary B cells *in vitro*.

Measles infections in humans cause a loss of antibody repertoire after recovery from measles [19] and vaccination was not associated with immunosuppression. Though there is loss in viability in uninfected primary B cells during culture, infected cultures have a significantly higher level of cell death ( $p < 0.05$ ). FL-15 infected cultures, had 1.6 times more cell death than EZ-GFP infected cultures at 48 h, suggesting that wild-type virus may induce more cell death in B cells. Increased B cell death may impact MeV induced immunosuppression by contributing to lymphopenia and alterations in the number of antigen specific cells within the B cell repertoire, both of which may be masked through the expansion of measles specific adaptive immune cells in response to infection.<sup>7,10,15,16</sup> The evaluation of cell death in B cell subtypes is subject to the limitation of higher frequency of naive cells detected in the periphery and lower frequency of memory cells which leads to more variability within the small cell population available for viability analysis. Our observations suggest that infection of B cells is not solely sufficient to induce changes in memory populations since immunosuppression is not observed following vaccination. Measles infection may induce differential cytokine profiles that lead to higher degrees of cell death *in vivo* or changes in signaling profiles that effect the survival and reconstitution of B cell populations.

Ferrets vaccinated with influenza vaccine and subsequently infected with canine distemper virus (CDV), a lymphotropic and immunosuppressive morbillivirus, showed a decrease in vaccine specific antibodies for up to 3 months, and the inability to respond to influenza challenge, suggesting functional changes in addition to repertoire changes following morbillivirus infection.<sup>10</sup> The hypothesis that changes in the function of B cells occurs during measles infection may be supported by the timing of viral clearance (20 days post infection in rhesus macaque model) and recovery from lymphopenia (within 3 months) compared to the extended immune suppression that can reach estimated time frames of several years.<sup>7,28,29</sup> Extended immune suppression suggests that other mechanisms beyond cell loss may contribute to functional changes within B cells.<sup>7,10</sup> The impact on B cell function observed following morbillivirus infection in ferrets<sup>10</sup> combined with the off-target effects contributing to the inability to respond to challenge, suggest that understanding the impact of wild-type MeV infection on antibody secreting cells present in the bone marrow and cells involved in the formation and function of germinal centers should be investigated. A limitation of our study is the inability to assess plasma cells and cells undergoing the germinal center reaction due to unavailability in peripheral blood.

Functional changes affecting B cells and other surrounding immune cells, could result from altered cytokine production. In rhesus macaques infected with wild-type MeV, viral RNA is detectable for several months after the clearance of viremia and the lack of IL-10 production has been associated with viral persistence in LCMV infections.<sup>29,30</sup> Lower levels of IL-10 production in FL-15 infected B cells could contribute to the persistence of MeV RNA.<sup>31</sup> EZ-GFP infected B cells produced higher levels of the pro-inflammatory cytokine TNF- $\alpha$  than FL-15 infected cells. These results suggest that a differential balance in pro-inflammatory and anti-inflammatory cytokines could influence B cell function during FL-15 infection. TNF- $\alpha$  has been linked to B cell survival signaling; higher levels of TNF- $\alpha$  expression in EZ-GFP infected B cells could contribute to B cell survival and the absence of selected loss of infected cells during vaccination.<sup>32</sup> Elevated IL-8 in FL-15 infected cells may result from binding of MeV-H to TLR-2,<sup>33,34</sup> which can induce IL-8 signaling in peripheral B cells.<sup>33-35</sup> Furthermore, the increased level of IL-8 following FL-15 infection could affect cellular chemotaxis, including of B cells, which may impact B cell reconstitution following MeV infection *in vivo*.<sup>36,37</sup> Unlike the cytokines discussed above, IL-4 and IL-6 are not differentially produced in FL-1 and EZ-GFP infected B cells, but they may tip the scales to the more characteristic pro-inflammatory route observed in EZ-GFP infected B cells compared to FL-15 infected cells. The cytokine evaluation was performed on a limited number of donors and therefore may not be generalizable; however, increased cell survival in EZ-GFP infected B cells supports the increased expression of TNF- $\alpha$  and thus survival in these infected cultures. *In vitro* cytokine evaluation as shown here may highlight potential targets of interest for *in vivo* analyses to assess the impact of cytokine expression on non-measles specific memory cells and antibody secreting cells.

The infection of B cells *in vitro* with a representative wild-type (FL-15) and vaccine (EZ-GFP) strain of MeV characterized here supports the widespread impact of MeV infection on B cell subtypes and the antibody repertoire. Comparison of infection with vaccine and wild-type infected cells highlighted differences that could contribute to the immune consequences demonstrated following measles. Cytokine production by EZ-GFP infected cells suggested a more canonical anti-viral response, while FL-15 infection could have implications in MeV RNA persistence and expansion of regulatory cells. Furthermore, while vaccine virus was spread more efficiently in B cells, wild-type infected cells showed significantly higher levels of cell death. Our studies suggest that both cell death and differential cytokine signaling may contribute to alterations in the B cell response and extended modulation of the immune response after viral clearance.

### Limitations of the study

In this study, we characterized infection of primary B cells with wild-type and vaccine strains of MeV. Vaccine-infected B cells had a higher percentage of cells expressing viral protein, a higher level of viral transcription and reduced cell death compared to wild-type infected cells. However, this study has several limitations. Logistical and financial constraints limited the number of B cell donors that could be tested. Because of the lower total cell numbers in the memory compartments compared to the naive B cell compartment in the periphery, greater variability was noted in memory B cells when assessing cell death. Future analyses could be performed using memory specific cell sorting methods to allow greater numbers of cells per subtype to be obtained. Because of low frequency in the periphery, it was not possible to measure infections in plasma cells or germinal center cells. However, our results do inform future studies to address measles infection of these target cells in by providing potential pathways to investigate in an *in vivo* model.

**STAR★METHODS**

Detailed methods are provided in the online version of this paper and include the following:

- **KEY RESOURCES TABLE**
- **RESOURCE AVAILABILITY**
  - Lead contact
  - Materials availability
  - Data and code availability
- **EXPERIMENTAL MODEL AND STUDY PARTICIPANT DETAILS**
  - Cell lines and primary cells
- **METHOD DETAILS**
  - Cell lines
  - Primary B cell isolation and culture
  - Virus preparation
  - Flow cytometry
  - Preparation of RNA
  - Detection of viral N gene via real-time PCR
  - Production of progeny virus
  - Cytokine analysis
- **QUANTIFICATION AND STATISTICAL ANALYSIS**

**SUPPLEMENTAL INFORMATION**

Supplemental information can be found online at <https://doi.org/10.1016/j.isci.2023.107721>.

**ACKNOWLEDGMENTS**

We would like to thank the Oak Ridge Institute for Science and Education for providing funding. We would also like to thank Dr. Jan Vinje for providing aliquots of the BJAB cell line and Dr. Paul Duprex for providing the GFP expressing EZ virus. We would like to thank Zachary Matson for providing support performing the multiplex bead assay to evaluate measles specific antibodies produced in the supernatant of infected cultures. We would also like to acknowledge BioRender for use of their software to produce the graphical abstract.

Disclaimer: The findings and conclusions in this report are those of the authors and do not necessarily represent the official position of the US Centers for Disease Control and Prevention nor Emory University.

**AUTHOR CONTRIBUTIONS**

L. M.: Conceptualization, methodology, validation, formal analysis, investigation, writing - original draft, writing - review and editing, visualization.

B.B.: Resources, writing - review and editing.

P.A.R.: Conceptualization, resources, supervision, writing - review and editing.

M.C.: Conceptualization, supervision, visualization, project administration, writing - review and editing.

**DECLARATION OF INTERESTS**

Authors have no declaration of competing interests to disclose.

Received: November 11, 2022

Revised: April 14, 2023

Accepted: August 22, 2023

Published: August 25, 2023

**REFERENCES**

1. Hutchins, S.S., Papania, M.J., Amler, R., Maes, E.F., Grabowsky, M., Bromberg, K., Glasgow, V., Speed, T., Bellini, W.J., and Orenstein, W.A. (2004). Evaluation of the measles clinical case definition. *J. Infect. Dis.* *189*, S153–S159. <https://doi.org/10.1086/379652>.
2. Salama, P., Assefa, F., Talley, L., Spiegel, P., van Der Veen, A., and Gotway, C.A. (2001). Malnutrition, measles, mortality, and the humanitarian response during a famine in Ethiopia. *JAMA* *286*, 563–571. <https://doi.org/10.1001/jama.286.5.563>.
3. Wolfson, L.J., Strebel, P.M., Gacic-Dobo, M., Hoekstra, E.J., McFarland, J.W., and Hersh, B.S.; Measles Initiative (2007). Has the 2005 measles mortality reduction goal been achieved? A natural history modelling study. *Lancet* *369*, 191–200. [https://doi.org/10.1016/s0140-6736\(07\)60107-x](https://doi.org/10.1016/s0140-6736(07)60107-x).
4. Dixon, M.G., Ferrari, M., Antoni, S., Li, X., Portnoy, A., Lambert, B., Hauryski, S., Hatcher, C., Nedelec, Y., Patel, M., et al. (2021). Progress Toward Regional Measles Elimination - Worldwide, 2000–2020. *MMWR Morb. Mortal. Wkly. Rep.* *70*, 1563–1569. <https://doi.org/10.15585/mmwr.mm7045a1>.

5. Lemon, K., de Vries, R.D., Mesman, A.W., McQuaid, S., van Amerongen, G., Yüksel, S., Ludlow, M., Rennick, L.J., Kuiken, T., Rima, B.K., et al. (2011). Early target cells of measles virus after aerosol infection of non-human primates. *PLoS Pathog.* 7, e1001263. <https://doi.org/10.1371/journal.ppat.1001263>.
6. Nelson, A.N., Putnam, N., Hauer, D., Baxter, V.K., Adams, R.J., and Griffin, D.E. (2017). Evolution of T Cell Responses during Measles Virus Infection and RNA Clearance. *Sci. Rep.* 7, 11474. <https://doi.org/10.1038/s41598-017-10965-z>.
7. Mina, M.J., Metcalf, C.J.E., de Swart, R.L., Osterhaus, A.D.M.E., and Grenfell, B.T. (2015). Long-term measles-induced immunomodulation increases overall childhood infectious disease mortality. *Science* 348, 694–699. <https://doi.org/10.1126/science.aaa3662>.
8. Singh, B.K., Li, N., Mark, A.C., Mateo, M., Cattaneo, R., and Sinn, P.L. (2016). Cell-to-Cell Contact and Nectin-4 Govern Spread of Measles Virus from Primary Human Myeloid Cells to Primary Human Airway Epithelial Cells. *J. Virol.* 90, 6808–6817. <https://doi.org/10.1128/JVI.00266-16>.
9. Mühlebach, M.D., Mateo, M., Sinn, P.L., Prüfer, S., Uhlrig, K.M., Leonard, V.H.J., Navaratnarajah, C.K., Frenze, M., Wong, X.X., Sawatsky, B., et al. (2011). Adherens junction protein nectin-4 is the epithelial receptor for measles virus. *Nature* 480, 530–533. <https://doi.org/10.1038/nature10639>.
10. Mina, M.J., Kula, T., Leng, Y., Li, M., de Vries, R.D., Knip, M., Siljander, H., Rewers, M., Choy, D.F., Wilson, M.S., et al. (2019). Measles virus infection diminishes preexisting antibodies that offer protection from other pathogens. *Science* 366, 599–606. <https://doi.org/10.1126/science.aay6485>.
11. Gadroen, K., Dodd, C.N., Masclee, G.M.C., de Ridder, M.A.J., Weibel, D., Mina, M.J., Grenfell, B.T., Sturkenboom, M.C.J.M., van de Vijver, D.A.M.C., and de Swart, R.L. (2018). Impact and longevity of measles-associated immune suppression: a matched cohort study using data from the THIN general practice database in the UK. *BMJ Open* 8, e021465. <https://doi.org/10.1136/bmjopen-2017-021465>.
12. Romanets-Korbut, O., Kovalevska, L.M., Seya, T., Sidorenko, S.P., and Horvat, B. (2016). Measles virus hemagglutinin triggers intracellular signaling in CD150-expressing dendritic cells and inhibits immune response. *Cell. Mol. Immunol.* 13, 828–838. <https://doi.org/10.1038/cmi.2015.55>.
13. de Vries, R.D., Lemon, K., Ludlow, M., McQuaid, S., Yüksel, S., van Amerongen, G., Rennick, L.J., Rima, B.K., Osterhaus, A.D.M.E., de Swart, R.L., and Duprex, W.P. (2010). In vivo tropism of attenuated and pathogenic measles virus expressing green fluorescent protein in macaques. *J. Virol.* 84, 4714–4724. <https://doi.org/10.1128/jvi.02633-09>.
14. de Vries, R.D., McQuaid, S., van Amerongen, G., Yüksel, S., Verburgh, R.J., Osterhaus, A.D.M.E., Duprex, W.P., and de Swart, R.L. (2012). Measles Immune Suppression: Lessons from the Macaque Model. *PLoS Pathog.* 8, e1002885. <https://doi.org/10.1371/journal.ppat.1002885>.
15. Laksono, B.M., de Vries, R.D., Verburgh, R.J., Visser, E.G., de Jong, A., Fraaij, P.L.A., Ruijs, W.L.M., Nieuwenhuijse, D.F., van den Ham, H.-J., Koopmans, M.P.G., et al. (2018). Studies into the mechanism of measles-associated immune suppression during a measles outbreak in the Netherlands. *Nat. Commun.* 9, 4944. <https://doi.org/10.1038/s41467-018-07515-0>.
16. Petrova, V.N., Sawatsky, B., Han, A.X., Laksono, B.M., Walz, L., Parker, E., Pieper, K., Anderson, C.A., de Vries, R.D., Lanzavecchia, A., et al. (2019). Incomplete genetic reconstitution of B cell pools contributes to prolonged immunosuppression after measles. *Sci. Immunol.* 4, eaay6125. <https://doi.org/10.1126/sciimmunol.aay6125>.
17. Beck, M., Smerdel, S., Dedić, I., Delimar, N., Rajninger-Miholic, M., Juzbasić, M., Manhalter, T., Vlatković, R., Borčić, B., and Mihajić, Z. (1986). Immune response to Edmonston-Zagreb measles virus strain in monovalent and combined MMR vaccine. *Dev. Biol. Stand.* 65, 95–100.
18. Brown, K.E., Rota, P.A., Goodson, J.L., Williams, D., Abernathy, E., Takeda, M., and Mulders, M.N. (2019). Genetic Characterization of Measles and Rubella Viruses Detected Through Global Measles and Rubella Elimination Surveillance, 2016–2018. *MMWR Morb. Mortal. Wkly. Rep.* 68, 587–591. <https://doi.org/10.15585/mmwr.mm6826a3>.
19. Organization, W.H. (2015). Genetic diversity of wild-type measles viruses and the global measles nucleotide surveillance database (MeaNS). *Wkly. Epidemiol. Rec.* 373–380.
20. Williams, D., Penedos, A., Bankamp, B., Anderson, R., Hübschen, J., Ben Mamou, M., Beck, A., Brown, D., Rey-Benito, G., Evans, R., et al. (2022). Update: circulation of active genotypes of measles virus and recommendations for use of sequence analysis to monitor viral transmission. *Weekly Epidemiological Record* 39.
21. Wu, Y.-C.B., Kipling, D., and Dunn-Walters, D.K. (2011). The Relationship between CD27 Negative and Positive B Cell Populations in Human Peripheral Blood. *Front. Immunol.* 2, 81. <https://doi.org/10.3389/fimmu.2011.00081>.
22. Laksono, B.M., Grosse-Wagener, C., de Vries, R.D., Langeveld, S.A.G., Brem, M.D., van Dongen, J.J.M., Katsikis, P.D., Koopmans, M.P.G., van Zelm, M.C., and de Swart, R.L. (2018). In Vitro Measles Virus Infection of Human Lymphocyte Subsets Demonstrates High Susceptibility and Permissiveness of both Naive and Memory B Cells. *J. Virol.* 92, e00131-18. <https://doi.org/10.1128/jvi.00131-18>.
23. Weller, S., Braun, M.C., Tan, B.K., Rosenwald, A., Cordier, C., Conley, M.E., Plebani, A., Kumararatne, D.S., Bonnet, D., Tournilhac, O., et al. (2004). Human blood IgM "memory" B cells are circulating splenic marginal zone B cells harboring a predifferentiated immunoglobulin repertoire. *Blood* 104, 3647–3654. <https://doi.org/10.1182/blood-2004-01-0346>.
24. Cerutti, A., Cols, M., and Puga, I. (2013). Marginal zone B cells: virtues of innate-like antibody-producing lymphocytes. *Nat. Rev. Immunol.* 13, 118–132. <https://doi.org/10.1038/nri3383>.
25. Singh, B.K., Pfaller, C.K., Cattaneo, R., and Sinn, P.L. (2019). Measles Virus Ribonucleoprotein Complexes Rapidly Spread across Well-Differentiated Primary Human Airway Epithelial Cells along F-Actin Rings. *mBio* 10, e02434-19–e02419. <https://doi.org/10.1128/mBio.02434-19>.
26. Koethe, S., Avota, E., and Schneider-Schaulies, S. (2012). Measles virus transmission from dendritic cells to T cells: formation of synapse-like interfaces concentrating viral and cellular components. *J. Virol.* 86, 9773–9781. <https://doi.org/10.1128/jvi.00458-12>.
27. Nguyen, D.T., de Witte, L., Ludlow, M., Yüksel, S., Wiesmann, K.H., Geijtenbeek, T.B.H., Osterhaus, A.D.M.E., and de Swart, R.L. (2010). The synthetic bacterial lipopeptide Pam3CSK4 modulates respiratory syncytial virus infection independent of TLR activation. *PLoS Pathog.* 6, e1001049. <https://doi.org/10.1371/journal.ppat.1001049>.
28. Tamashiro, V.G., Perez, H.H., and Griffin, D.E. (1987). Prospective study of the magnitude and duration of changes in tuberculin reactivity during uncomplicated and complicated measles. *Pediatr. Infect. Dis. J.* 6, 451–454. <https://doi.org/10.1097/00006454-198705000-00007>.
29. Nelson, A.N., Lin, W.H.W., Shivakoti, R., Putnam, N.E., Mangus, L., Adams, R.J., Hauer, D., Baxter, V.K., and Griffin, D.E. (2020). Association of persistent wild-type measles virus RNA with long-term humoral immunity in rhesus macaques. *JCI Insight* 5, e134992. <https://doi.org/10.1172/jci.insight.134992>.
30. Richter, K., Perriard, G., and Oxenius, A. (2013). Reversal of chronic to resolved infection by IL-10 blockade is LCMV strain dependent. *Eur. J. Immunol.* 43, 649–654. <https://doi.org/10.1002/eji.201242887>.
31. Lin, W.H.W., Kouyos, R.D., Adams, R.J., Grenfell, B.T., and Griffin, D.E. (2012). Prolonged persistence of measles virus RNA is characteristic of primary infection dynamics. *Proc. Natl. Acad. Sci. USA* 109, 14989–14994. <https://doi.org/10.1073/pnas.1211138109>.
32. Bousiotis, V.A., Nadler, L.M., Strominger, J.L., and Goldfeld, A.E. (1994). Tumor necrosis factor alpha is an autocrine growth factor for normal human B cells. *Proc. Natl. Acad. Sci. USA* 91, 7007–7011. <https://doi.org/10.1073/pnas.91.15.7007>.
33. Bieback, K., Lien, E., Klagge, I.M., Avota, E., Schneider-Schaulies, J., Duprex, W.P., Wagner, H., Kirschning, C.J., Ter Meulen, V., and Schneider-Schaulies, S. (2002). Hemagglutinin protein of wild-type measles virus activates toll-like receptor 2 signaling. *J. Virol.* 76, 8729–8736. <https://doi.org/10.1128/jvi.76.17.8729-8736.2002>.
34. Agrawal, S., and Gupta, S. (2011). TLR1/2, TLR7, and TLR9 Signals Directly Activate Human Peripheral Blood Naive and Memory B Cell Subsets to Produce Cytokines, Chemokines, and Hematopoietic Growth Factors. *J. Clin. Immunol.* 31, 89–98. <https://doi.org/10.1007/s10875-010-9456-8>.
35. Ganley-Leal, L.M., Liu, X., and Wetzler, L.M. (2006). Toll-like receptor 2-mediated human B cell differentiation. *Clin. Immunol.* 120, 272–284. <https://doi.org/10.1016/j.clim.2006.04.571>.
36. Baggolini, M., and Clark-Lewis, I. (1992). Interleukin-8, a chemotactic and inflammatory cytokine. *FEBS Lett.* 307, 97–101. [https://doi.org/10.1016/0014-5793\(92\)80909-z](https://doi.org/10.1016/0014-5793(92)80909-z).
37. Jinquan, T., Møller, B., Storgaard, M., Mukaida, N., Bonde, J., Grunnet, N., Black,

- F.T., Larsen, C.G., Matsushima, K., and Thestrup-Pedersen, K. (1997). Chemotaxis and IL-8 receptor expression in B cells from normal and HIV-infected subjects. *J. Immunol.* 158, 475–484.
38. Ono, N., Tatsuo, H., Hidaka, Y., Aoki, T., Minagawa, H., and Yanagi, Y. (2001). Measles viruses on throat swabs from measles patients use signaling lymphocytic activation molecule (CDw150) but not CD46 as a cellular receptor. *J. Virol.* 75, 4399–4401. <https://doi.org/10.1128/jvi.75.9.4399-4401.2001>.
39. Rennick, L.J., de Vries, R.D., Carsillo, T.J., Lemon, K., van Amerongen, G., Ludlow, M., Nguyen, D.T., Yüksel, S., Verburch, R.J., Haddock, P., et al. (2015). Live-attenuated measles virus vaccine targets dendritic cells and macrophages in muscle of nonhuman primates. *J. Virol.* 89, 2192–2200. <https://doi.org/10.1128/jvi.02924-14>.
40. Lei, C., Yang, J., Hu, J., and Sun, X. (2021). On the Calculation of TCID<sub>50</sub> for Quantitation of Virus Infectivity. *Virol. Sin.* 36, 141–144. <https://doi.org/10.1007/s12250-020-00230-5>.
41. Hummel, K.B., Lowe, L., Bellini, W.J., and Rota, P.A. (2006). Development of quantitative gene-specific real-time RT-PCR assays for the detection of measles virus in clinical specimens. *J. Virol. Methods* 132, 166–173. <https://doi.org/10.1016/j.jviromet.2005.10.006>.
42. Ramakrishnan, M.A. (2016). Determination of 50% endpoint titer using a simple formula. *World J. Virol.* 5, 85–86. <https://doi.org/10.5501/wjv.v5.i2.85>.

## STAR★METHODS

### KEY RESOURCES TABLE

REAGENT or RESOURCE	SOURCE	IDENTIFIER
<b>Antibodies</b>		
mouse blend anti-measles virus hemagglutinin (CV1/CV4)	MilliporeSigma™	Cat#MAB8905; RRID: AB_95486
mouse monoclonal phycoerythrin conjugated anti-human CD27	BD Pharmigen™	Cat#555441; RRID: AB_395834
mouse monoclonal allophycocyanin conjugated anti-human CD19	BD Pharmigen™	Cat#555415; RRID: AB_398597
mouse monoclonal BD™ Horizon Brilliant Ultraviolet (BUV) 395 conjugated anti-human CD20	BD Horizon™	Cat#563782
mouse monoclonal Alexa 700 conjugated anti-human IgD	BD Pharmigen™	Cat#561302
mouse monoclonal BD Brilliant Violet (BV) 605 conjugated anti-human CD24	BD Horizon™	Cat#562788
mouse monoclonal BV786 conjugated anti-human CD38	BD Horizon™	Cat#563964
Zombie Violet viability stain	Biolegend™	Cat#423113
F(ab') <sub>2</sub> -Goat anti-Mouse IgG (H + L) polyclonal secondary antibody, FITC	eBioscience™	Cat#11-4010-82; RRID: AB_2572490
<b>Bacterial and virus strains</b>		
Lab passaged Edmonston Zagreb with GFP insertion (EZ-GFP)	Dr. Paul Duprex <sup>39</sup>	N/A
Lab passaged D8 (FL-15)	Clinical isolate MVs/Florida.USA/12.15	N/A
<b>Biological samples</b>		
Fresh human blood	Emory Donor Services	N/A
Frozen peripheral B cells	STEMCell™ Technologies	Cat#70023
<b>Critical commercial assays</b>		
Qiagen™ RNeasy Mini Kits	Qiagen™	Cat#74104
QIAamp™ Viral RNA	Qiagen™	Cat#52904
SuperScript™/Taq polymerase SuperScript™ III Platinum™ One-Step qRT-PCR kit	Invitrogen™	Cat#11732020
Cytokine 10-Plex Human Panel	ThermoFisher™	Cat# LHC0001M
pan human B cell isolation kit	Miltenyi Biotec™	Cat#130-101-638
<b>Experimental models: Cell lines</b>		
BJAB cell line	Dr. Jan Vinje, Centers for Disease Control and Prevention	
Vero/hSLAM cell line	Yusuke Yanagi, MD, PhD Kyushu University, Fukuoka, Japan <sup>38</sup>	
<b>Oligonucleotides</b>		
Measles virus N forward primer 5'-ATTACATCAGGATCCGG-3'	Integrated DNA Technologies <sup>41</sup>	<a href="https://www.idtdna.com">https://www.idtdna.com</a>
Measles virus N reverse primer 5'-GTATTGGTCCGCCTCATC-3'	Integrated DNA Technologies <sup>41</sup>	<a href="https://www.idtdna.com">https://www.idtdna.com</a>

(Continued on next page)

**Continued**

REAGENT or RESOURCE	SOURCE	IDENTIFIER
Rnase P forward primer 5'-AGATTTGGACCTGCGAGCG-3'	Integrated DNA Technologies <sup>41</sup>	<a href="https://www.idtdna.com">https://www.idtdna.com</a>
Rnase P reverse primer 5'-GAGCGGCTGTCTCCACAAGT-3'	Integrated DNA Technologies <sup>41</sup>	<a href="https://www.idtdna.com">https://www.idtdna.com</a>
<b>Software and algorithms</b>		
FlowJo™	N/A	<a href="https://www.flowjo.com/">https://www.flowjo.com/</a>
Graphpad™ Prism	N/A	<a href="https://www.graphpad.com/">https://www.graphpad.com/</a>

**RESOURCE AVAILABILITY****Lead contact**

Further information and requests for resources and reagents should be directed toward and will be fulfilled by the lead contact, Logan Melot ([lmelot@emory.edu](mailto:lmelot@emory.edu)).

**Materials availability**

This study did not generate new unique reagents.

**Data and code availability**

- Data reported in this paper can be shared by the [lead contact](#) upon request.
- This paper does not report original code.
- Any additional information required to reanalyze the data reported in this paper is available from the [lead contact](#) upon request.

**EXPERIMENTAL MODEL AND STUDY PARTICIPANT DETAILS****Cell lines and primary cells**

Cell lines used consisted of Vero/hSLAM cells and BJAB cells. Vero/hSLAM cells are Vero (*Chlorocebus sabaeus*, kidney cells, NCBI Taxonomy 60711) cells and stably transfected with human SLAMF1.<sup>38</sup> These cells were isolated from a female African green monkey. Cells were passaged or maintained until passage 30 at 37°C DMEM supplemented with 10% heat-inactivated fetal bovine serum (HI-FBS) 0.4 mg/mL Geneticin (G418) (Gibco, 10131035), 1% penicillin-streptomycin, and 1% L-glutamine). BJAB cells are an EBV negative human Burkitt lymphoma cell line. These cells were isolated from a female. BJAB cells were passaged or maintained until passage 30 at 37°C in RPMI (10% HI-FBS, 1% penicillin-streptomycin, and 1% L-glutamine). Cell lines have been authenticated through ATCC.

Primary cell cultures consisted of B cells isolated from healthy human donor blood (CDC IRB Protocol #1652) by sequential gradient centrifugation and negative selection using Miltenyi Biotec MACS LS columns or frozen cells provided by STEMCell technologies. Frozen cells were stored at -180°C before being thawed for infection and analysis. During culture B cells were maintained in RPMI medium (5% HI-FBS, 1% penicillin-streptomycin, 1% L-glutamine, 50 μM 2-mercaptoethanol) at 37°C. Average age of all donors was 51 years of age with a range of 28–64 years of age. Both fresh and frozen cells were isolated from an individual of each sex.

**METHOD DETAILS****Cell lines**

Vero/hSLAM cells were passaged or maintained in DMEM supplemented with 10% heat-inactivated fetal bovine serum (HI-FBS) 0.4 mg/mL Geneticin (G418) (Gibco, 10131035), 1% penicillin-streptomycin, and 1% L-glutamine.<sup>38</sup> BJAB cells (non-EBV Burkitt-lymphoma B cell line provided by Dr. Jan Vinje's lab at Centers for Disease Control and Prevention) were cultured in RPMI (10% HI-FBS, 1% penicillin-streptomycin, and 1% L-glutamine).

**Primary B cell isolation and culture**

Whole blood from healthy human donors was collected in heparin tubes (CDC IRB Protocol #1652). Peripheral blood mononuclear cells (PBMCs) were isolated by gradient centrifugation with Lymphocyte Separation Medium (Corning, 25-072-CV). Blood was centrifuged for 30 min at room temperature at 400 x g without break. Remaining red blood cells were lysed with Ammonium-Chloride-Potassium (ACK) lysing buffer (Gibco, A1049201). PBMC counts isolated from donors averaged  $2.08 \times 10^6 \pm 0.64$  ( $1.08-3.16 \times 10^6$ ) per mL of freshly isolated whole blood. B cells were isolated by negative selection using a pan human B cell isolation kit (Miltenyi Biotec, 130-101-638) and purity (88–97%) was measured via flow cytometry (Figure S1). B cells were counted, and 250,000 cells were seeded in 96 well round-bottom plates in RPMI medium (5% HI-FBS, 1% penicillin-streptomycin, 1% L-glutamine, 50 μM 2-mercaptoethanol). Frozen B cells (STEMCell Technologies, 70023) were

stored in liquid nitrogen at  $-180^{\circ}\text{C}$  before being thawed for infection and analysis, PBMC isolation counts for these donors was not obtained by supplier. Average age of all donors was 51 years of age with a range of 28–64 years of age.

### Virus preparation

Cells were infected with either a low passage wild-type MeV, MVs/Florida.USA/12.15 [D8] (FL-15) or a recombinant EZ virus containing a GFP reporter gene inserted after the measles P gene (EZ-GFP).<sup>39</sup> All viral stocks were prepared by infecting Vero/hSLAM cells for 72 h (MOI  $<0.01$ ,  $32^{\circ}\text{C}$ ) in DMEM (2% HI-FBS, 1% penicillin-streptomycin, 1% L-glutamine, 0.2 mg/mL G418). Cells were harvested, lysed by freeze-thaw, supernatant was clarified by centrifugation (1500 RPM,  $4^{\circ}\text{C}$ ) for 5 min and aliquoted. Viral titer was determined by 0.5% crystal violet staining of a plaque assay after 6 days incubation in Vero/hSLAM cells using 2% carboxymethylcellulose (CMC) overlay (FL-15 =  $2.1 \times 10^7$ , EZ-GFP =  $1.1 \times 10^8$ ). Plaque-forming units per mL were calculated for each virus stock. Virus stock was UV inactivated at 2000 mW/cm<sup>2</sup> on ice for 4 h (EZ and FL-15) or 8 h (EZ-GFP). UV inactivation was confirmed by TCID<sub>50</sub>.<sup>40</sup>

BJAB cells or primary B cells were seeded into a 96-well round-bottom plate at 250,000 cells per well. Cells were pelleted by centrifugation at 1500 RPM for 10 min at  $4^{\circ}\text{C}$ . Cells were infected at an MOI of 1 by resuspension of cell pellet in virus containing RPMI (5% HI-FBS, 1% penicillin-streptomycin, 1% L-glutamine, and 50  $\mu\text{M}$  2-mercaptoethanol) and incubated at  $37^{\circ}\text{C}$ . Infected cells were then pelleted at timepoints via centrifugation at 1500 RPM for 10 min at  $4^{\circ}\text{C}$  and were washed with PBS (no  $\text{Mg}^{2+}$ ,  $\text{Ca}^{2+}$ ) before further analysis.

### Flow cytometry

Viral protein expression in B cells was analyzed by flow cytometry using a BD LSRFortessa flow cytometer (BD Biosciences). Vaccine was detected through GFP expression and wild-type cells were detected using MeV hemagglutinin (H) protein by antibody staining using mouse anti-H (MilliporeSigma, MAB8905, clone CV1/CV4) and anti-mouse IgG fluorescein isothiocyanate (FITC) conjugated secondary antibody (eBioscience, 11-4010-82). Immunophenotyping of B cells was performed using phycoerythrin conjugated anti-CD27 (BD Pharmigen, 555441), allophycocyanin conjugated anti-CD19 (BD Pharmigen, 555415), BD Horizon Brilliant Ultraviolet (BUV) 395 conjugated anti-CD20 (BD Horizon, 563782), Alexa 700 conjugated anti-IgD (BD Pharmigen, 561302), BD Brilliant Violet (BV) 605 conjugated anti-CD24 (BD Horizon, 562788), BV786 conjugated anti-CD38 (BD Horizon, 563964), and Zombie Violet viability stain (Biolegend, 423113). Positive fluorescent values were determined as signal above the isotype control for each fluorophore. Positive values for viral fluorescence were determined as the signal above cells stained for viral protein expression at 0 h.

### Preparation of RNA

Cells were pelleted by centrifugation (1500 RPM,  $4^{\circ}\text{C}$ ) for 10 min. Cell pellets were homogenized using Qiashredder spin columns (Qiagen, 79656). RNA was isolated from infected cells using Qiagen RNeasy Mini Kits (Qiagen, 74104) according to the manufacturer's instructions at 0-, 24-, and 48-h after infection. Viral lysates used for infection were also assessed for presence of residual viral RNA using a QIAamp Viral RNA kit according to manufacturer's instructions (Qiagen, 52904). Messenger RNA (mRNA) was preferentially amplified using oligo(dT)12–18 primers and SuperScript III (Invitrogen, 18080044) reverse transcriptase according to manufacturer's recommendation. Samples were incubated with RNase H (500 ng/ $\mu\text{L}$ ) (Invitrogen, 18021014) for 30 min at  $37^{\circ}\text{C}$  to remove residual RNA.

### Detection of viral N gene via real-time PCR

Real-time PCR (rRT-PCR) was performed using an Applied Biosystems 7500 Fast Real-time PCR System. MeV N gene was detected using Taqman primers and probes using SuperScript/Taq polymerase SuperScript III Platinum One-Step qRT-PCR kit (Invitrogen, 11732020) as previously described.<sup>41</sup> Samples were incubated at  $48^{\circ}\text{C}$  for 30 min and  $95^{\circ}\text{C}$  for 5 min, followed by cycling ( $95^{\circ}\text{C}$  for 15 s,  $60^{\circ}\text{C}$  for 1 min) 40 times. MeV N detection was normalized to a housekeeping gene, RNaseP (RPPH1).

### Production of progeny virus

Infected cells were pelleted by centrifugation at 1500 RPM for 10 min at  $4^{\circ}\text{C}$ . Supernatant was collected and cells were resuspended in media equivalent to supernatant media at 250  $\mu\text{L}$  and placed at  $-80^{\circ}\text{C}$  for 24 h to lyse the cells. Supernatants and cellular lysates from infected B cells were titrated on Vero/hSLAM cells in DMEM (2% HI-FBS, 1% penicillin-streptomycin, 1% L-glutamine, 0.2 mg/mL G418) using an 8 point 10-fold serial dilution curve and incubated for 6 days at  $37^{\circ}\text{C}$ . Cells were stained with crystal violet, TCID<sub>50</sub>/mL was calculated by the Reed-Muench method and converted to PFU/mL by multiplying by a factor of 0.7.<sup>42</sup>

### Cytokine analysis

Cytokines were measured using a Luminex FlexMap3D instrument (BioRad Laboratories). Supernatants from infected B cells were analyzed using a 10-plex human cytokine panel to assess GM-CSF, IL-1 $\beta$ , IL-2, IL-4, IL-5, IL-6, IL-8, IL-10, IFN- $\gamma$ , and TNF- $\alpha$  protein production (ThermoFisher, LHC0001M). Protein concentration was determined using the manufacturer provided standard.

### QUANTIFICATION AND STATISTICAL ANALYSIS

Flow cytometry data were collected from the BD LSRFortessa using FACSDiva software and analyzed using FlowJo version 10. The n listed in the figure legends represents individual infections. Statistical analysis by multiple t-tests to compare differences in means of percent positive cells from 0 to 24 h, 0 to 48 h, and 24 to 48 h was performed using Graphpad Prism version 8. MeV N gene expression measured by rRT-PCR was normalized to RNaseP (RPPH1) and the  $2^{-\Delta C_t}$  calculated. Statistical analysis by multiple t-test to compare MeV N gene expression at 0 to 24 h, 0 to 48 h and 24 to 48 h was performed using Graphpad Prism version 8. Cytokine MFI was converted to pg/mL concentration using the included standard according to manufacturer's recommendations. Increases in cytokine concentration were determined by subtracting detectable cytokine at 0-h timepoints. Statistical analyses for cytokine production were performed to determine differences between infection with EZ-GFP compared to infection with FL-15 or changes within each condition between 24- and 48-hours-post-infection. Differences were checked for significance using multiple t-tests.